Theoretical Study of Cytosine Deamination from the Perspective of the Reaction Force Analysis

Vanessa Labet,[†] Christophe Morell,[†] André Grand,[†] and Alejandro Toro-Labbé*[,‡]

Laboratoire "Lésions des Acides Nucléiques", INAC/SCIB - UMR-E no. 3 CEA-UJF, CEA Grenoble, 17 avenue des Martyrs, F-38054 Grenoble cedex 9, France, and Laboratorio de Química Teórica Computacional (QTC), Facultad de Química, Pontifica Universidad Católica de Chile, Casilla 306, Correo 22, Santiago, Chile

Received: July 4, 2008; Revised Manuscript Received: September 5, 2008

A theoretical study of two different mechanisms for the spontaneous deamination of cytosine is presented. In the first mechanism, a tetrahedral intermediate results in a two-step mechanism whereas in the second one, it is the result of a concerted step. In this work a link is made between the two pathways through the study of the evolution along the reaction coordinates of chemical concepts such as chemical potential, hardness and electronic populations within the framework of the reaction force analysis. The reaction force profile suggests that the concerted mechanism is composed of two asynchronous events. The observation of the reaction force profile appears as an easy way to identify asynchronous concerted steps and as a privileged tool to study the more or less asynchronous character of chemical reactions.

1. Introduction

In a recent computational study, Almatarneh et al.[1] explored the hydrolytic deamination of cytosine in the gas phase by nucleophilic attack of either a hydroxyl anion or a water molecule, by means of HF/6-31G(d), MP2/6-31G(d), B3LYP/6-31G(d) and G3MP2 levels of theory. A total of four different pathways were explored, two with a water molecule as the nucleophilic reagent, and two others with a hydroxyl anion. In the two cases where a water molecule is involved, the creation of a covalent link between the water oxygen and carbon C4 of the cytosine appears as the rate-determining step. Figure 1 sketches the formation of this covalent bond in the more favorable of the two pathways. First of all, there is tautomerization of the canonical cytosine with assistance of a water molecule (**R1-TS1_1-I1_1**), followed by the nucleophilic attack of this water molecule on carbon C4 with simultaneous proton transfer from H_2O to the exocyclic imine nitrogen of cytosine to form the tetrahedral intermediate (**I1_1-TS2_1-I2_1**).

More recently, Labet et al.[2] studied the hydrolytic deamination of cytosine in the gas phase and in aqueous solvent by nucleophilic attack of a water molecule on either the canonical cytosine or its N3-protonated form, by means of DFT/6-311G(d,p) and PCM/DFT/6-311G(d,p) levels of theory. They proposed a mechanism involving two water molecules, a first one that plays the role of the nucleophilic reagent, and a second one that assists the first one. In this study too, the nucleophilic attack of the water molecule appears as the rate-determining step. Figure 2 sketches the C−O bond formation in the case where the substrate is the canonical cytosine. The tetrahedral intermediate is the same as the one involved in the mechanism proposed by Almatarneh et al.[1] (except the fact that it is in interaction with one water molecule) and the single step giving its formation from the canonical cytosine in interaction with two water molecules (**R_2-TS1_2-I1_2**) involves a concerted process and a six-centers transition state. It looks like a combination of the two elementary steps involved in the mechanism of Almatarneh et al.[1] Figure 3 presents the optimized geometries of the stationary points involved in the formation of the tetrahedral intermediate in the two mechanisms. The associated thermodynamic and kinetic parameters are reported in Table 1 and the energetics scheme is shown in Figure 4.

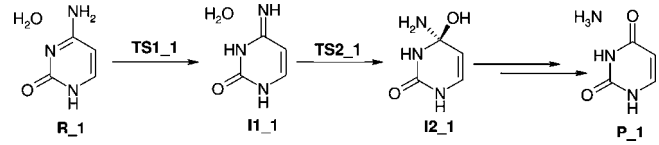

Figure 1. Sketch of the beginning of the reaction pathway for the deamination of cytosine with one water molecule, proposed by Almatarneh et al.[1]

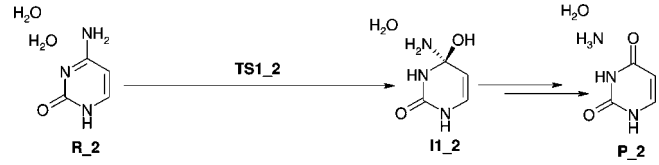

Figure 2. Sketch of the beginning of the reaction pathway for the deamination of cytosine with two water molecules, proposed by Labet et al.[2]

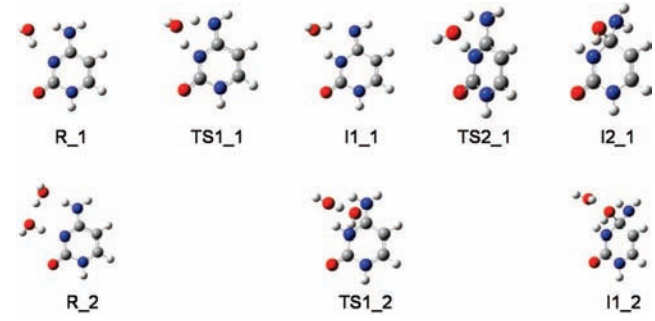

Figure 3. Geometries of the stationary points involved in the first part (C−O bond creation) of the deamination of cytosine with one and two water molecules, optimized at B3LYP/6-311G(d,p) level of theory.

[†] Laboratoire "Lésions des Acides Nucléiques".
[‡] Pontifica Universidad Católica de Chile.

10.1021/jp8059097 CCC: $40.75
Published on Web 10/18/2008

TABLE 1: Thermodynamic and Kinetic Parameters for the First Part (C−O Bond Creation) of the Deamination of Cytosine with One and Two Water Molecules at Standard Conditions (298.15 K and 1 atm) in the Gas Phase[a]

	R_1-TS1_1-I1_1	I1_1-TS2_1-I2_1	R_2-TS1_2-I1_2
$\Delta_r E^{\ddagger}$	52.2	209.4	148.3
$\Delta_r E$	9.3	57.0	89.0
$\Delta_r H^{\ddagger}$	52.2	209.4	148.3
$\Delta_r H$	9.3	57.0	89.0
$\Delta_r G^{\ddagger}$	61.1	214.0	162.1
$\Delta_r G$	10.8	62.1	94.1

[a] All values are in kJ/mol and calculated at the B3LYP/6-311G(d,p) level of theory.

To compare these two propositions, the mechanism of Almatarneh et al.[1] has been calculated at the B3LYP/6-311G(d,p) level of theory and then characterized within the framework of the reaction force analysis.[3] A tentative correlation is made between the evolution of chemical concepts such as energy, reaction force, chemical potential and hardness, and the evolution of structural parameters and electronic properties as bond distances and Mulliken atomic populations along the reaction path. We will focus particularly on the **R_2-TS1_2-I1_2** step and on its relation with the two others. Section 2 will be devoted to the presentation of the concepts used for the analysis of the three elementary steps. In section 3, the way as the results have been obtained will be detailed. Then, section 4 will present the results and the discussion.

2. Theoretical Background

2.1. Energy. For a generic elementary step along the reaction coordinate ξ, the potential energy $E(\xi)$ presents a universal form: it increases from the reactant(s) to the transition state and decreases from the transition state to the product(s). Reactant(s) and product(s) correspond to a relative minimum of energy whereas the transition state corresponds to a maximum of energy. The relative position of these extrema provides kinetic and thermodynamic information of the chemical reaction.

2.2. Reaction Force. The concept of reaction force was introduced a few years ago by Toro-Labbé.[3] It is defined as

$$F(\xi) = -\frac{dE}{d\xi} \tag{1}$$

where ξ is the reaction coordinate that measures the reaction progress when going from reactants to products. It represents the force acting on the system to bring the reactant(s) into the product(s). As the potential energy, the reaction force presents a universal form along the reaction coordinate. For an elementary step it exhibits a minimum between the reactant and the transition state (corresponding to the inflection point in the activation part of the potential energy) and a maximum between the transition state and the product (corresponding to the inflection point in the relaxation part of the potential energy). These particular points define the transition state region, which is mainly characterized by bond breaking and forming processes, and correspond to transitions between different stages of the elementary step.[3−10]

2.3. Chemical Potential and Hardness. Chemical potential (μ) and absolute hardness (η) are global electronic indices that provide information about the reactivity of a molecular system. Within the conceptual density functional theory, they have been defined as[11−13]

$$\mu = \left(\frac{\partial E}{\partial N}\right)_{v(\vec{r})} \qquad \eta = \frac{1}{2}\left(\frac{\partial^2 E}{\partial N^2}\right)_{v(\vec{r})} \tag{2}$$

Chemical potential measures the escaping tendency of the electronic cloud from equilibrium[14] and the absolute hardness the resistance to charge transfer.[15−17]

3. Method and Computational Details

All calculations were performed using the Gaussian 03 package.[18] Calculations along the reaction coordinate were performed at the B3LYP[19,20]/6-311G(d,p)[21−23] level of theory, in the gas phase through the intrinsic reaction coordinate procedure[24] from the geometry of the transition state fully optimized at the B3LYP/6-311G(d,p), and checked by a vibrational analysis at the same level of theory. The profiles of energy, reaction force, chemical potential, hardness, structural parameters and electronic properties were obtained through single-point calculations on the previously optimized geometries given by the IRC procedure.

The chemical potential and absolute hardness were calculated using a finite difference approximation and the Koopmans' theorem, i.e., using the following formulas:[11,25]

$$\mu \approx \frac{1}{2}(\varepsilon_{LUMO} + \varepsilon_{HOMO}) \qquad \eta \approx \frac{1}{2}(\varepsilon_{LUMO} - \varepsilon_{HOMO}) \tag{3}$$

where ε_{HOMO} and ε_{LUMO} are the energies of the highest occupied and the lowest unoccupied molecular orbitals, HOMO and LUMO, respectively.

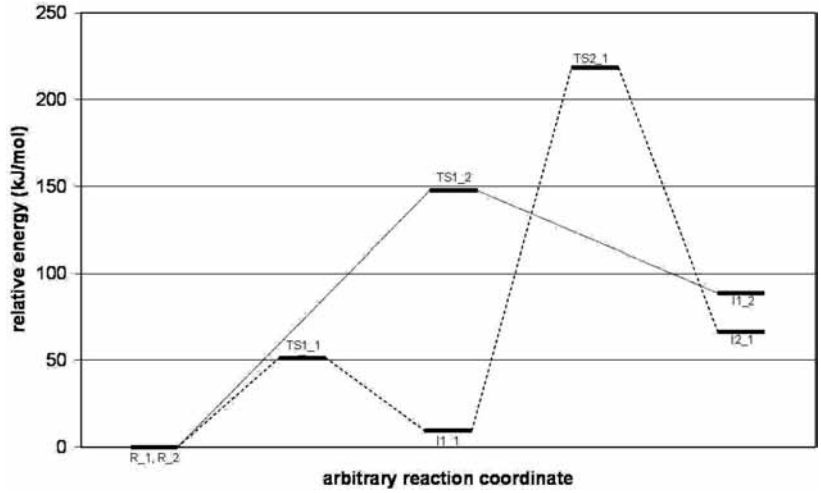

Figure 4. Energetics of the first part (C−O bond creation) of the deamination of cytosine with one and two water molecules.

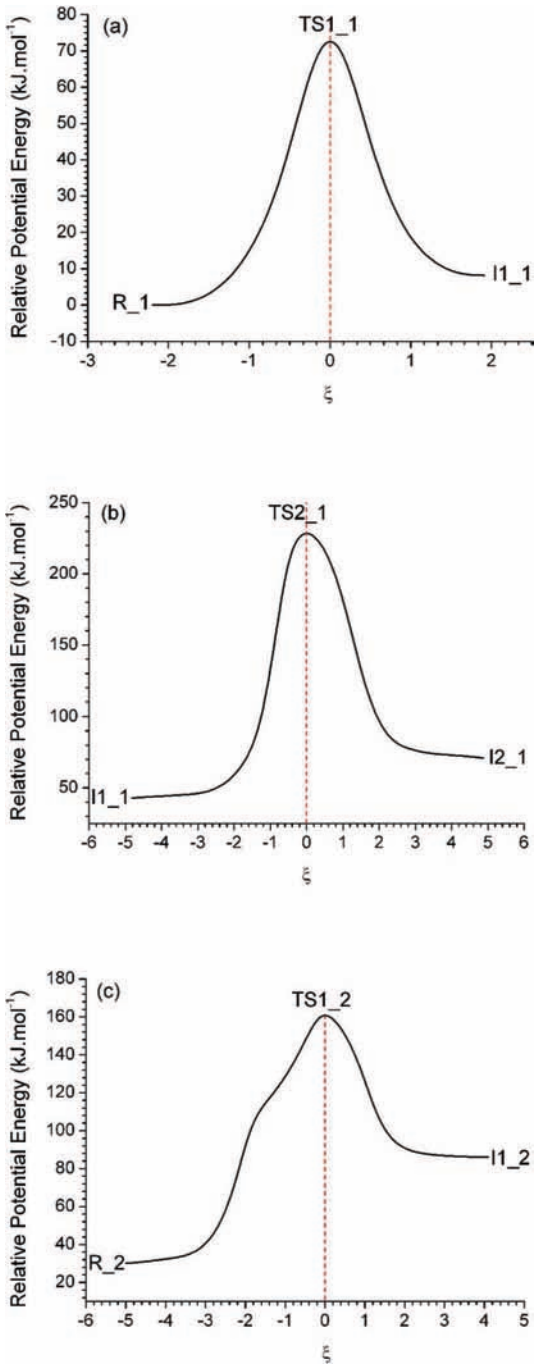

Figure 5. Relative potential energy (in kJ mol^{-1}) along the IRC for the three elementary steps involved in the deamination of cytosine with one and two water molecules: (a) **R_1-TS1_1-I1_1**; (b) **I1_1-TS2_1_I2_1**; (c) **R_2-TS1_2-I1_2**.

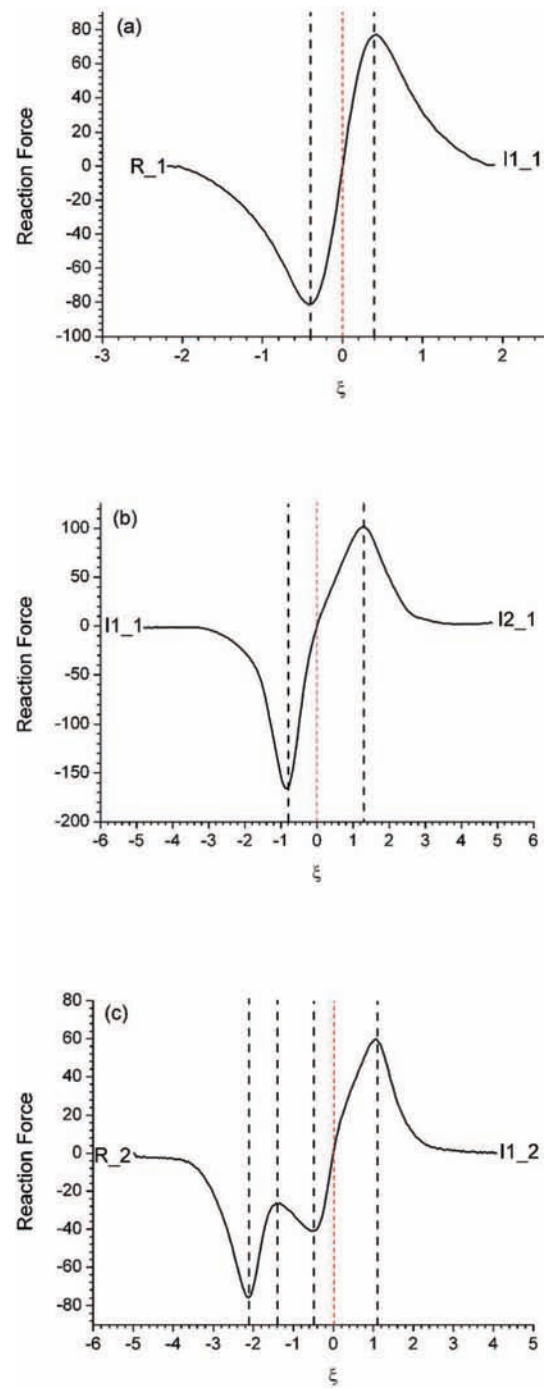

Figure 6. Reaction force (corresponding to an energy in kJ mol^{-1}) along the IRC for the three elementary steps involved in the deamination of cytosine with one and two water molecules: (a) **R_1-TS1_1-I1_1**; (b) **I1_1-TS2_1_I2_1**; (c) **R_2-TS1_2-I1_2**. The red dashed lines indicate the position of the transitions states, and the black ones the limits of the different regions identified along the reaction coordinate.

4. Results and Discussion

4.1. Energetic Analysis. The potential energy profiles along the intrinsic reaction coordinate for the two first steps of the deamination of cytosine with one water molecule, and for the first step of the deamination of cytosine with two water molecules are represented in Figure 5. Whereas the two energy profiles of Figure 5a,b have the classical form of an elementary step with an inflection point before the transition state and one after, it is different for the energy profile of Figure 5c, which presents a shoulder before the energy maximum. Although only one transition state connects **R_2** and **I1_2**, this suggests that the corresponding "elementary" step seems to be the composition of two simpler processes.

4.2. Reaction Force Profile. As already mentioned in section 2.2, during an elementary step, the reaction force presents a minimum and a maximum at the two inflection points of the potential energy. Between these two extrema, the reaction force vanishes one time at the transition state. This profile for the reaction force, which is the one that can be observed in Figure 6a,b, is universal. The difference between the different kinds of elementary steps comes from a rise and a fall that are more or less symmetric, more or less deep and more or less wide. Indeed, during the cytosine tautomerization assisted by a water

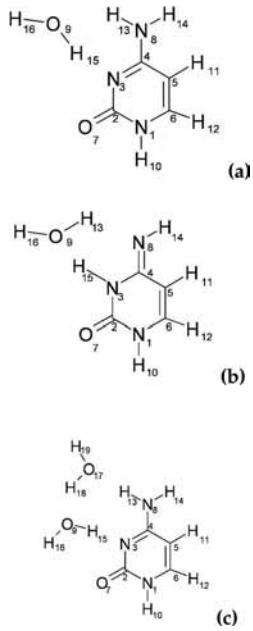

Figure 7. Atomic numbering used for the elementary steps description: (a) **R_1-TS1_1-I1_1**; (b) **I1_1-TS2_1-I2_1**; (c) **R_2-TS1_2-I1_2**.

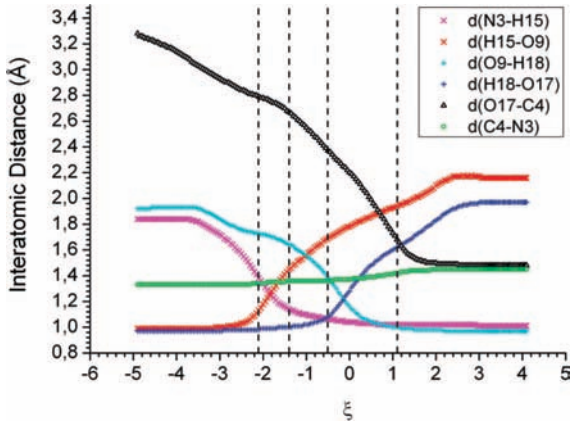

Figure 8. Evolution of the distances mainly affected during the **R_2-TS1_2-I1_2** step.

molecule, the activation and relaxation parts of the reaction force are quite symmetric with each other. It can be explained by the symmetric character of this reaction, which involves two proton transfers, one from the exocyclic amine nitrogen of cytosine to the oxygen of a water molecule, and one from this latter oxygen to nitrogen N3 of cytosine. On the contrary, during the following step, corresponding to the nucleophilic addition of a water molecule on carbon C4 of the cytosine tautomer, the relaxation part of the reaction force is less deep and wider than the activation part.

Similarly, during the first step of the deamination of cytosine with two water molecules, the reaction force vanishes at the transition state, but it presents an unexpected local maxima before the transition state ($\xi = -1.4$), corresponding to the shoulder in the associated potential energy profile (Figure 5c). From **R_2** to **I1_2**, the reaction force goes through two local minima ($\xi = -2.1$ and $\xi = -0.5$) and two local maxima ($\xi = -1.4$ and $\xi = 1.1$). This seems to confirm the fact that this elementary step is composed of two events and that it is their simultaneity that leads to only one energy barrier and a unique transition state. It can be supposed that the second minimum is

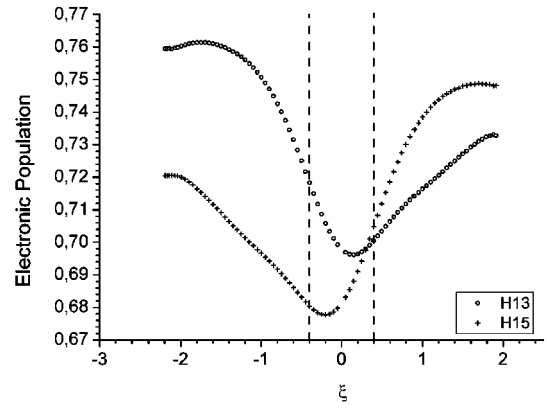

Figure 9. Evolution of the electronic population on H13 and H15 along the reaction path of the **R_1-TS1_1-I1_1** elementary step.

not as deep as the first one because of the superposition of the relaxation part of the first event and the activation part of the second one.

Moreover, it can be noticed that for the two nucleophilic addition steps (the one with a single water molecule (**I1_1-TS2_1-I2_1**, Figure 6b), and the one with two water molecules (**R_2-TS1_2-I1_2**, Figure 6c)) the relaxation parts of the reaction force are very similar in terms of shape, although the intensity is smaller in the case of the deamination with two water molecules, in accordance with the fact that the assisted nucleophilic addition is more endothermic than the nonassisted one. About the profile in the reactant region (before the first minima), the one for the tautomerization step (**R_1-TS1_1-I1_1**, Figure 6a), and the one for the assisted nucleophilic addition step (**R_2-TS1_2-I1_2**, Figure 6c) look the same in terms of shape and intensity. This suggests the fact that during the complex **R_2-TS1_2-I1_2** step, the first process looks like the tautomerization whereas the second one is the nucleophilic addition properly speaking. This will be confirmed in the next section by examination of the evolution of several structural parameters during the **R_2-TS1_2-I1_2** step.

4.3. Evolution of Structural Parameters. Figure 7 presents the atomic numbering used in the following discussion for each elementary step. During the first step of the deamination of cytosine with two water molecules, H15 is transferred from O9 to N3, H18 from O17 to O9, a C−O bond is created between O17 and C4 and the C4−N3 double bond is transformed into a single one. Figure 8 presents the evolution of the distances mainly affected by this reaction, i.e., *d*(N3−H15), *d*(H15−O9), *d*(O9−H18), *d*(H18−O17), *d*(O17−C4) and *d*(C4−N3). It can be noticed that before $\xi = -4$, all these distances are constant except the one between O17 and C4, that is, the distance between the cytosine and the water molecule which plays the role of assistant in the nucleophilic addition. Although this change in the relative orientation of the two molecules is not really part of the reaction, it prepares it for the forthcoming events. After $\xi = 3$ all the distances remained fixed. Consequently, it can be considered that the reaction takes place between $\xi = -4$ and $\xi = 3$, which is consistent with the domain of variation of the reaction force (Figure 6c).

Between $\xi = -4$ and $\xi = -3$, the distances between N3 and H15 and between O9 and H18 decrease without any increase of the distances between O9 and H15 and between O17 and H18. The three reactants are coming closer each other without any charge transfer. Then, between $\xi = -3$ and $\xi = -1$, the distance between N3 and H15 continues to decrease whereas the distance between O9 and H15 increases. This phase

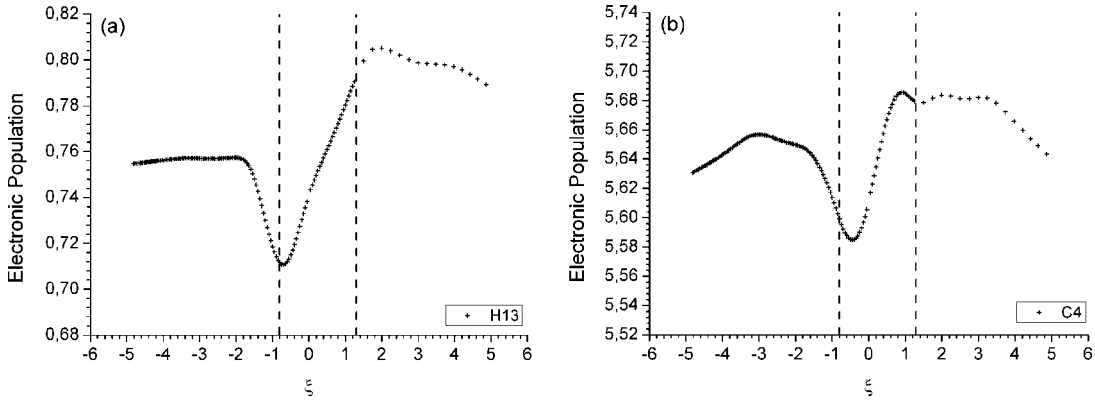

Figure 10. Evolution of the electronic population on H13 (a) and on C4 (b) along the reaction path of the **I1_1-TS2_1-I2_1** elementary step.

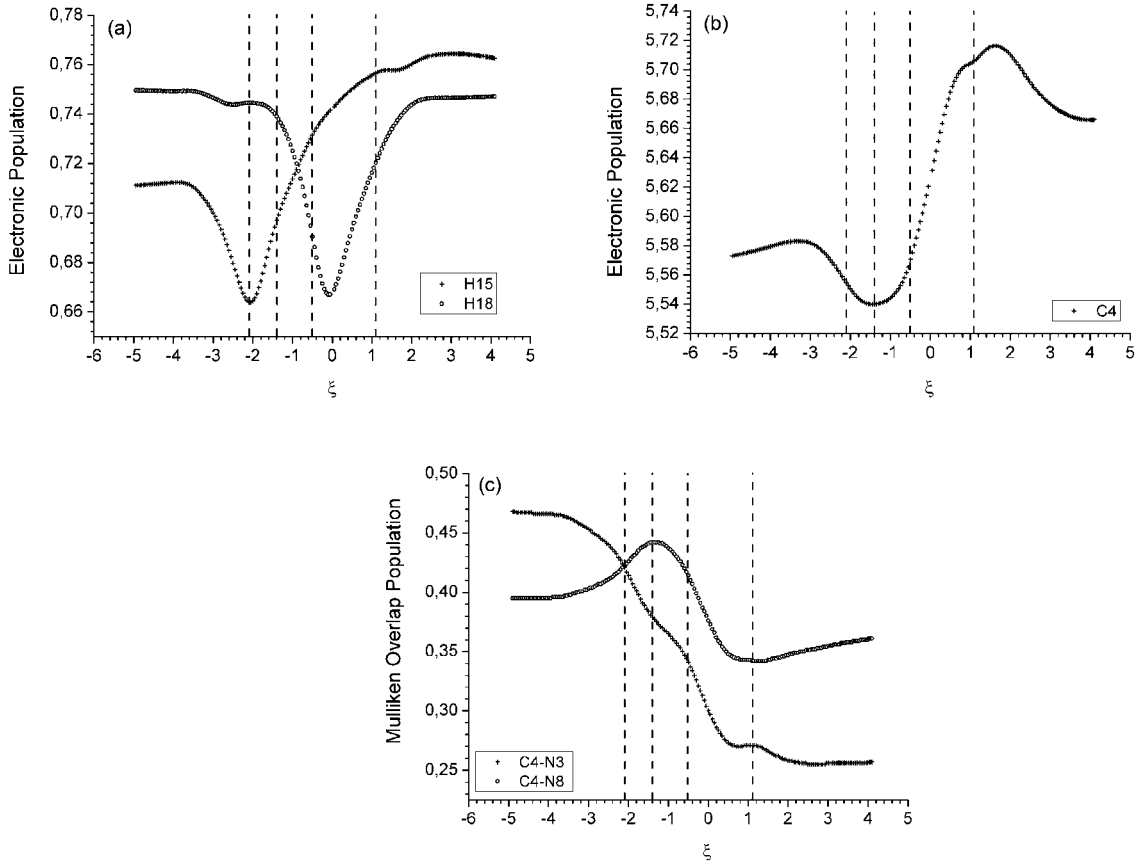

Figure 11. Evolution of the electronic population on H15 and H18 (a) and on C4 (b) and evolution of the overlap populations between C4 and N3 and between C4 and N8 (c) along the reaction path of the **R_2-TS1_2-I1_2** elementary step.

corresponds to the beginning of H15 transfer from O9 to N3, i.e., the process that looks like the **R_1-TS1_1-I1_1** tautomerization step. In the same domain of reaction coordinate, the distance between O17 and H18 remains constant whereas the distance between O9 and H18 decreases, indicating that the transfer of H18 from O17 to O9 has not yet begun.

Indeed, H18 is transferred between $\xi = -1$ and $\xi = 1$. After $\xi = 1$, the transfers of H18 and H15 are achieved because the distances between O9 and H18, and between N3 and H15 are constant. The increase of the distance between O17 and H18 and between O9 and H15 correspond to the removal of the products. The distance between O17 and C4 decreases regularly before $\xi = -2$ and more deeply between $\xi = -2$ and $\xi = 2$ with a simultaneous increase of the C4−N3 bond length. The formation of the C4−O17 bond can be considered to occur between $\xi = -2$ and $\xi = 2$.

From these considerations, the first local minima of the reaction force during the **R_2-TS1_2-I1_2** step can be associated with the activation of the H15 transfer from O9 to N3 whereas a link can be established between the second minimum, located at $\xi = -0.5$, and the activation of the H18 transfer from O17 to O9. The study of the electronic reordering during the **R_2-TS1_2-I1_2** step will help to precise this point.

4.4. Electronic Reordering. Figure 9 presents the evolution of the electronic population on the two transferred hydrogen atoms along the reaction path of the **R_1-TS1_1-I1_1** elementary step. It appears that the two charge transfers are quasi synchronous. They take place between $\xi = -2$ and $\xi = +2$. Note that the symmetry of the reaction entails that the electronic population on H13 and H18 present minima just before and after the transition state, respectively. The domain between the force minimum and maximum is the domain where the charge transfer from one hydrogen

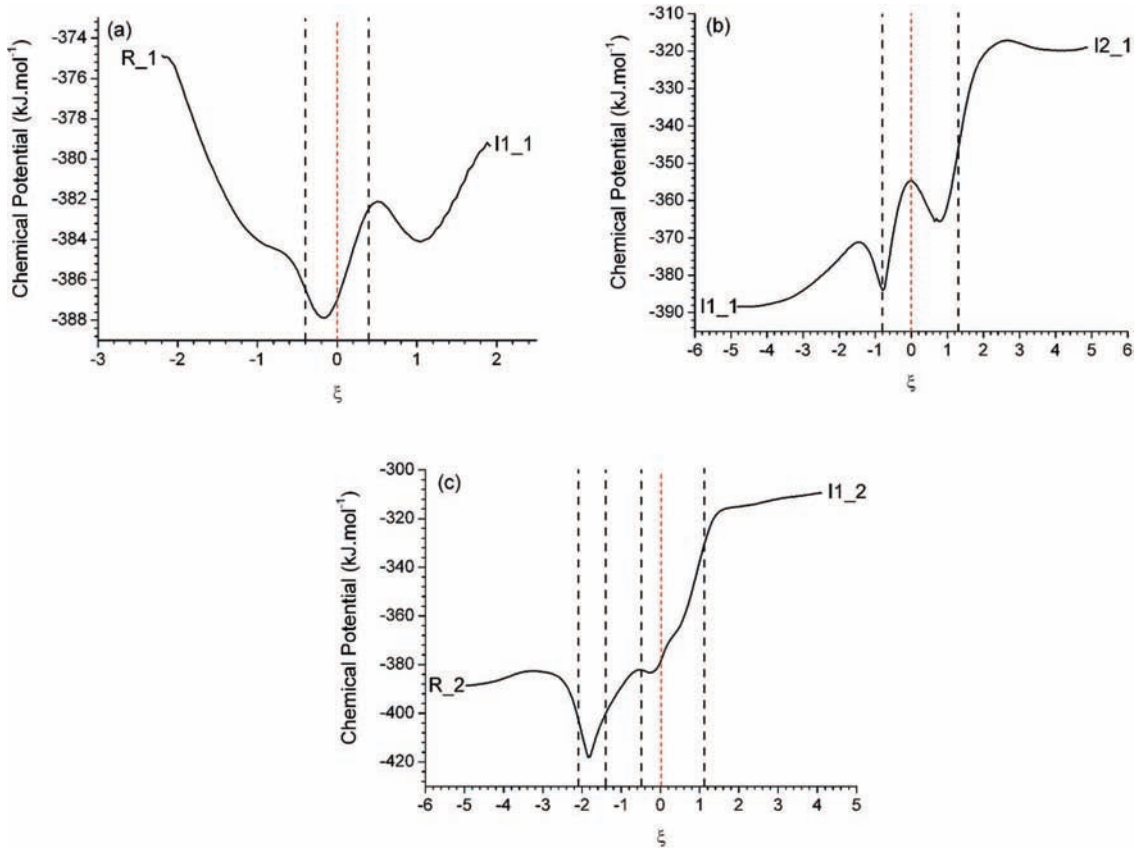

Figure 12. Chemical potential (in kJ mol^{-1}) along the IRC for the three elementary steps involved in the deamination of cytosine with one and two water molecules: (a) **R_1-TS1_1-I1_1**; (b) **I1_1-TS2_1_I2_1**; (c): **R_2-TS1_2-I1_2**.

to the other, due to the quasi synchronous O9−H15 bond breaking/O9−H13 bond creation, is localized.

Figure 10 presents the evolution of the electronic population on H13 and C4 along the reaction path of the **I1_1-TS2_1-I2_1** elementary step. H13 is the hydrogen that is transferred from the water molecule to the cytosine tautomer during the nucleophilic addition. C4 is the cytosine carbon that undergoes the nucleophilic attack. The two charge transfers associated to the proton transfer and the formation of the C−O covalent bond appears to be synchronous. It can be observed that within the transition state region the electronic population increases on both H13 and C4 because of the formation of the N8−H13 and C4−O9 bonds.

On Figure 11a is represented the evolution of the atomic populations for the two protons transferred during the step, i.e., H15 and H18. The trend is the same in both cases: the two populations decrease together with the O9−H15 and O17−H18 bond breakings and increase in line with the N3−H15 and O9−H18 bond formations. It appears that the charge transfer associated to the H18 atom transfer begins ($\xi = -2.0$) before the charge associated to H15 is transferred ($\xi = 2.5$), thus confirming the fact that the two proton transfers are asynchronous. The electronic populations on H15 and H18 are minimal at $\xi = -2.1$ and $\xi = -0.1$ respectively, close to the reaction force minima ($\xi = -2.1$ and $\xi = -0.5$). The electronic population on H15 in the **I1_2** region is larger than that in the **R_2** region because H15 is linked to a nitrogen atom in **I1_2** whereas it is linked to an oxygen atom in **R_2**. The two landing levels are quite similar for H18 because it belongs to a water molecule in the two molecular systems.

On Figure 11b is represented the evolution of the electronic population on carbon C4. Between $\xi = -3.3$ and $\xi = -1.4$, it decreases because of the H15 transfer from O9 to N3 to whom C4 is covalently linked. Then the C4−O17 bond formation increases the C4 population until $\xi = 1.6$. The evolution before $\xi = -3.3$ and after $\xi = 1.6$ can be attributed to a modification in the orientation of the reactants and products relative to each other. The formation of the C4−O10 bond appears quite synchronous with the H18 proton transfer from O17 to O9.

On Figure 11c is represented the evolution of the Mulliken overlap populations between C4 and N3 and between C4 and N8, which can be made in relation with the electronic populations of the C4−N3 and C4−N8 bonds respectively. Along the **R_2-TS1_2_I1_2** elementary step, the C4−N3 double bond is transformed into a single one. That is why the overlap population between C4 and N3 decreases along the reaction coordinate. As for the overlap population between C4 and N8, it can be noticed that it increases before the first local maximum ($\xi = -1.4$) in the reaction force and decreases until the second local maximum ($\xi = 1.1$). The increasing phase corresponds to the domain where the electronic population on C4 decreases. A fraction of electrons that were localized on C4 are transferred into the C4−N8 bond to decrease the electronic repulsion between carbon C4 and oxygen O17, which become closer. The decreasing phase corresponds to the formation of the C4−O17 bond. A fraction of the electrons of the C4−N8 bond participate in the formation of the C4−O17 one. An interesting point to be underlined is the fact that the crossing point of the two bonds population can be considered as the starting point of the whole reaction.

4.5. Chemical Potential and Hardness Profiles. During the three elementary steps studied in this work, the chemical potential passes through at least three critical points (Figure 12). A similar behavior for the chemical potential has already been

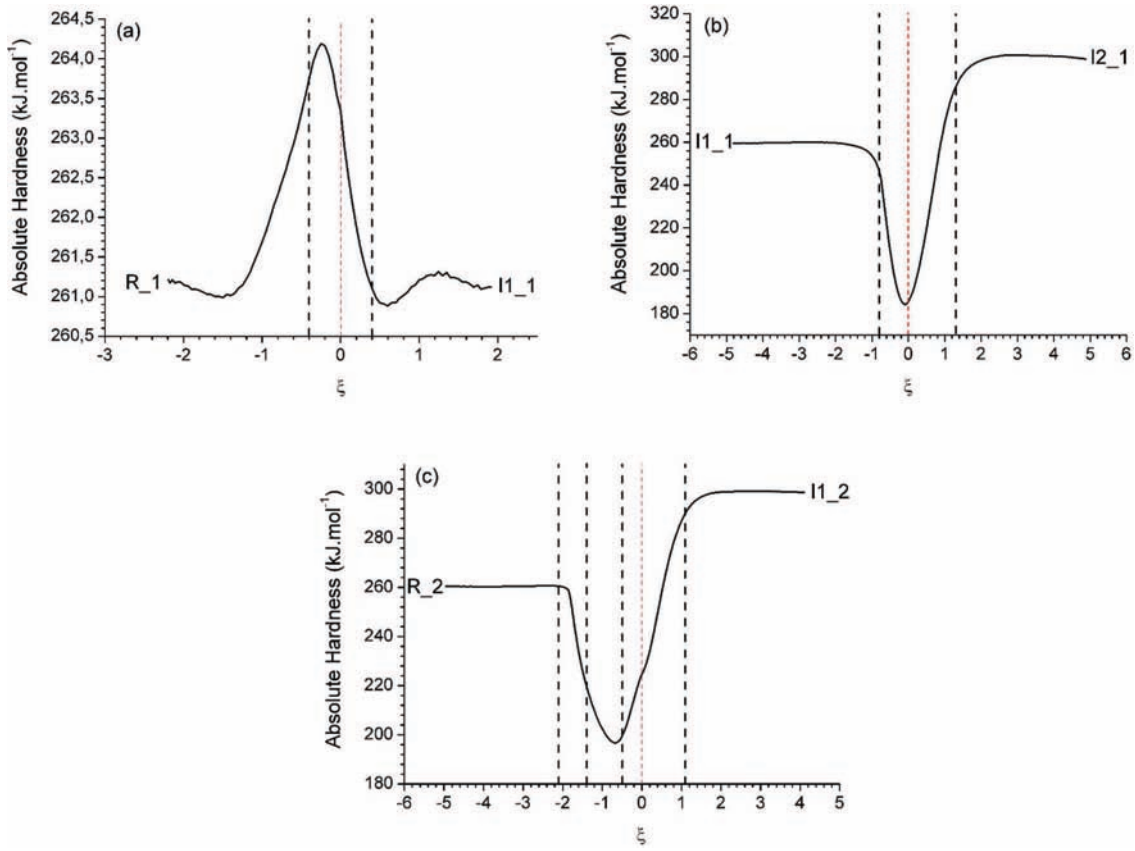

Figure 13. Absolute hardness (in kJ ol^{-1}) along the IRC for the three elementary steps involved in the deamination of cytosine with one and two water molecules: (a) **R_1-TS1_1-I1_1**; (b) **I1_1-TS2_1_I2_1**; (c) **R_2-TS1_2-I1_2**.

described in the literature.[4] It was suggested there that it was an indicator of specific interactions taking place in different regions of the reaction path (reactant, transition state, and product).

In the tautomerization step (Figure 12a), the chemical potential is minimal in the vicinity of the transition state. It is the reverse for the nonassisted nucleophilic addition step (Figure 12b) where the transition state corresponds to a relative maximum of chemical potential. The product of the tautomerization step has a smaller chemical potential (more negative) than its reactant. The cytosine tautomer appears more favorable to an electronic gain than the canonical cytosine, and is consequently a better candidate to a nucleophilic attack.

For the two nucleophilic addition steps (the nonassisted one, Figure 13b, and the assisted-one, Figure 13c) the molecular hardness reach a minimum at or near the transition state. A small shifting of the minimum toward the reactants is observed in the assisted nucleophilic addition; this can be an element suggesting that this step is more complicated than it seems to be.

It can be noticed that the molecular hardness presents small changes during the tautomerization step (±3 kJ/mol) (Figure 13a) whereas it varies dramatically (±100 kJ/mol) during the nonassisted nucleophilic addition step (Figure 13b). This can explain that the hardness profile for the assisted nucleophilic addition looks like the one for the nonassisted nucleophilic addition. It can also be an element for explaining that the principle of maximum hardness cannot be applied in the case of the tautomerization step.

The simultaneous observation of Figures 8, 9 and 13c indicates that in the case of the **R_2-TS1_2-I1_2** elementary step, the domain where the hardness varies a lot and is minimal corresponds to the domain where the nuclei are transferred. Indeed, the electronic population on H15 decreases after $\xi = -3.8$, the one on H18 increases until $\xi = 2.2$, and the absolute hardness varies a lot between $\xi = -2.0$ and $\xi = 1.8$.

5. Concluding Remarks

Concerning the deamination reaction of cytosine, a nucleophilic attack at the C4 position is not possible in its canonical form, and the increase of the electrophilic tendency of this carbon must be enhanced by a previous step of tautomerization, or by introducing an assistant water molecule. The mechanism in one step proposed here for the formation of the tetrahedral intermediate is asynchronous. It corresponds to the superposition of two events, one being the protonation of N3 (transfer of H15 from O9 to N3) and the second being the nucleophilic addition of a water molecule on C4 (transfer of H18 from O17 to O9 and creation of the C4−O17 bond).

Concerning the study of asynchronous concerted mechanisms, the reaction force appears to be a well adapted tool, presenting a great discrimination. That is the consequence of the universal character of its profile along the intrinsic reaction coordinate.

Acknowledgment. We thank financial support from CEA-Grenoble and from FONDECYT through project No. 1060590, FONDAP through project No. 11980002 (CIMAT).

References and Notes

(1) Almatarneh, M. H.; Flinn, C. G.; Poirier, R. A.; Sokalski, W. A. *J. Phys. Chem. A* **2006**, *110*, 8227–8234.
(2) Labet, V.; Grand, A.; Morell, C.; Cadet, J.; Eriksson, L. A. *Theor. Chem. Acc.*, in press.
(3) Toro-Labbé, A. *J. Phys. Chem. A* **1999**, *103*, 4398.

(4) Jaque, P.; Toro-Labbé, A. *J.Phys. Chem A* **2000**, *104*, 995.
(5) Toro-Labbé, A.; Gutiérrez-Oliva, S.; Concha, M. C.; Murray, J. S.; Politzer, P. *J. Chem. Phys.* **2004**, *121*, 4570.
(6) Herrera, B.; Toro-Labbé, A. *J. Chem. Phys.* **2004**, *121*, 7096.
(7) Gutiérrez-Oliva, S.; Herrera, B.; Toro-Labbé, A.; Chermette, H. *J. Phys. Chem. A.* **2005**, *109*, 1748.
(8) Politzer, P.; Toro-Labbé, A.; Gutiérrez-Oliva, S.; Herrera, B.; Jaque, P.; Concha, M. C.; Murray, J. *J. Chem. Sci.* **2005**, *117*, 467.
(9) Politzer, P.; Burda, J. V.; Concha, M. C.; Lane, P.; Murray, J. *J. Phys. Chem. A* **2006**, *110*, 756.
(10) Rincon, E.; Jaque, P.; Toro-Labbé, A. *J. Phys. Chem. A* **2006**, *110*, 9478.
(11) Parr, R. G.; Yang, W. *Density Functional Theory of Atoms and Molecules*; Oxford University Press: New York, 1989.
(12) Geerlings, P.; De Proft, F.; Langenaeker, W. *Chem. Rev.* **2003**, *103*, 1793.
(13) Parr, R. G.; Yang, W. *Annu. Rev. Phys. Chem.* **1995**, *46*, 701.
(14) Parr, R. G.; Donnelly, R. A.; Levy, M.; Palke, W. E. *J. Chem. Phys.* **1978**, *68*, 3801.
(15) Parr, R. G.; Pearson, R. G. *J. Am. Chem. Soc.* **1983**, *105*, 7512.
(16) Pearson, R. G. *J. Am. Chem. Soc.* **1985**, *107*, 6801.
(17) Pearson, R. G. *J. Chem. Educ.* **1987**, *64*, 561.
(18) Frisch, M. J.; Trucks, G. W.; Schlegel, H. B.; Scuseria, G. E.; Robb, M. A.; Cheeseman, J. R.; Montgomery, J. A., Jr.; Vreven, T.; Kudin, K. N.; Burant, J. C.; Millam, J. M.; Iyengar, S. S.; Tomasi, J.; Barone, V.; Mennucci, B.; Cossi, M.; Scalmani, G.; Rega, N.; Petersson, G. A.; Nakatsuji, H.; Hada, M.; Ehara, M.; Toyota, K.; Fukuda, R.; Hasegawa, J.; Ishida, M.; Nakajima, T.; Honda, Y.; Kitao, O.; Nakai, H.; Klene, M.; Li, X.; Knox, J. E.; Hratchian, H. P.; Cross, J. B.; Adamo, C.; Jaramillo, J.; Gomperts, R.; Stratmann, R. E.; Yazyev, O.; Austin, A. J.; Cammi, R.; Pomelli, C.; Ochterski, J. W.; Ayala, P. Y.; Morokuma, K.; Voth, G. A.; Salvador, P.; Dannenberg, J. J.; Zakrzewski, V. G.; Dapprich, S.; Daniels, A. D.; Strain, M. C.; Farkas, O.; Malick, D. K.; Rabuck, A. D.; Raghavachari, K.; Foresman, J. B.; Ortiz, J. V.; Cui, Q.; Baboul, A. G.; Clifford, S.; Cioslowski, J.; Stefanov, B. B.; Liu, G.; Liashenko, A.; Piskortz, P.; Komaromi, I.; Martin, R. L.; Fox, D. J.; Keith, T.; Al-Laham, M. A.; Peng, C. Y.; Nanayakkara, A.; Challacombe, M.; Gill, P. M. W.; Johnson, B.; Chem, W.; Wong, M. W.; Gonzalez, C.; Pople, J. A. *Gaussian 03*, revision C.02; Gaussian, Inc.: Wallingford, CT, 2004.
(19) Becke, A. D. *J. Chem. Phys.* **1993**, *98*, 5648–5652.
(20) Lee, C.; Yang, W.; Parr, R. G. *Phys. Rev. B.* **1988**, *37*, 785–789.
(21) McLean, A. D.; Chandler, G. S. *J. Chem. Phys.* **1980**, *72*, 5639.
(22) Krishnan, R.; Binkley, J. S.; Seeger, R.; Pople, J. A. *J. Chem. Phys.* **1980**, *72*, 650.
(23) Frisch, M. J.; Pople, J. A.; Binkley, J. S. *J. Chem. Phys.* **1984**, *80*, 3265.
(24) Fukui, K. *Acc. Chem. Res.* **1981**, *14*, 363.
(25) Parr, R. G.; Zhou, Z. *Acc. Chem. Res.* **1993**, *26*, 252.

JP8059097